Rapid Screening of Bimetallic Electrocatalysts for Oxygen Reduction in Acidic Media by Scanning Electrochemical Microscopy

Darren A. Walsh,* José L. Fernández, and Allen J. Bard**,z

Department of Chemistry and Biochemistry, University of Texas at Austin, Austin, Texas 78712, USA

Additional bimetallic electrocatalysts for the oxygen reduction reaction (ORR) in acidic media were designed using a previously reported thermodynamic selection guide. The electrocatalyst mixtures were prepared in large arrays on glassy carbon substrates and the electrocatalytic activity was screened using scanning electrochemical microscopy (SECM). Activities were measured for a range of bimetallic combinations that showed a synergetic electrocatalytic effect during screening, including Au–V, Ag–V, Pd–Mn, and Pd–V. Upon initial screening, a highly active electrocatalytic combination consisting of 60:40 Pd–V was identified. Using rotating disk electrode (RDE) experiments, the high activity of this combination for the ORR in acidic media was confirmed when the electrocatalysts were supported on Vulcan carbon. The electrocatalytic activity of Pd–V was close to that exhibited by Pt, the electrocatalyst of choice for the ORR in acidic media, and thus is another example of a nonplatinum catalyst with high activity that follows the previous strategy for catalyst design.
© 2006 The Electrochemical Society.   [DOI: 10.1149/1.2186208] All rights reserved.

Polymer electrolyte membrane fuel cells (PEMFCs) have been widely proposed as potentially inexpensive, efficient, and clean energy sources.[1-5] Research in this area is directed at a number of approaches, including the development of improved polymeric membrane materials,[6,7] nanocarbon electrode supports,[8-11] and the search for replacement cathode materials for the oxygen reduction reaction (ORR).[12,13] Of these, the latter is particularly important if PEMFCs are to achieve widespread application as the current Pt electrocatalysts are very expensive and even with Pt the nonideal kinetics for the ORR leads to significant overpotentials ($\sim$0.4 V) and power losses.[14,15] In an effort to reduce the quantity of Pt required for fuel cell applications, a range of Pt alloys has been reported that exhibits good activity for the ORR.[16-20] Despite this, replacement of the Pt in PEMFCs with a significantly less expensive non-Pt electrocatalyst in PEMFCs, and catalyst improvement for the ORR remain major goals in this field.

The search for novel electrocatalysts has benefited in recent years from the introduction of several rapid screening methods.[21-23] In particular, a method of automatically preparing test arrays of bimetallic ORR electrocatalyst spots on an inactive (glassy carbon) substrate followed by rapid scanning electrochemical microscopy (SECM) screening was recently described.[24] SECM screening involved the evolution of O_2 at a metal tip, which diffused to the array component immediately beneath the tip, where it was electroreduced. By holding the substrate at different potentials, it was possible to identify those mixtures with high activities for the ORR and to construct current-potential curves for the ORR reaction at that composition. The SECM screening method used very little material and was rapid, so it was possible to screen very large arrays of different bimetallic combinations rather quickly. The mixture components were selected using simple guidelines based on thermodynamic principles involving the so-called "direct route" of oxygen reduction, where one of the metals was selected for good dissociative chemisorption of O_2 onto the surface (metal 1, M), forming adsorbed oxygen atoms (O$^{\bullet}$) (e.g., $2M + O_2 \rightarrow 2MO$). Electroreduction of O$^{\bullet}$ at the surface by metal 2, M$'$, with the addition of 4 protons and 4 electrons, then results in the overall reduction of O_2 to H_2O ($2M'O + 4H^+ + 4e \rightarrow 2M' + 2H_2O$).[24] Bimetallic combinations were chosen that combined a metal that easily forms adsorbed O$^{\bullet}$ by breaking the O–O bond of O_2 (i.e., a highly negative free energy for metal oxide formation) with a second metal whose oxide is easy to reduce to water (i.e., a positive potential for metal oxide

reduction) as shown in Fig. 1, which extends the range of metals given previously.[24] The applicability of the selection guide and screening method was examined using combinations of Pd, Au, and Ag (as metal 2) with Co (as metal 1), and a reduction in the ORR overpotential was observed in each case. Therefore, the selection guide was a very useful starting point when deciding which systems to screen. Upon detection of promising electrocatalytic combinations, they can be studied in greater detail by preparing mixtures with carbon and examining by rotating disk electrode (RDE) voltammetry and then scaled up for testing under actual fuel cell conditions.

The work reported here extends the previous studies using the reported selection guide[24] by selecting metals that form metal oxides (i.e., break the O–O of O_2) more easily than Co, so that it might be possible to design bimetallic electrocatalysts that show better enhancement of the synergetic effect. In particular, this is illustrated using combinations that contain Mn and V. Each of these metals has large negative free energies for oxide formation (<-350 kJ mol^{-1}) and so readily form metal oxides. These metals have been combined with metals whose oxides are easily reducible (Au, Ag, and Pd) to test further the guidelines and search for enhanced ORR electrocatalysis at bimetallic spots containing these metals compared to the single metal. Significantly, an additional Pd-based combination that exhibits high activity for the ORR has been identified. RDE measurements confirm the high activity of this electrocatalyst and a comparison with commercial Pt electrocatalyst is described.

Experimental

Chemicals.— Glassy carbon (GC) plates (1 mm thick, 50 $\times$ 50 mm) were purchased from Alfa Aesar (Ward Hill, MA). Prior to use, the GC plates were cut into smaller squares to produce the substrates (15 $\times$ 15 mm). $(NH_4)_2PdCl_4$ (Aldrich), $HAuCl_4$ (Alfa), $AgNO_3$ (Aldrich), VCl_2 (Aldrich), and $Mn(NO_3)_2$ (Aldrich) were used as obtained and Milli-Q water was used to prepare all solutions. Vulcan carbon XC-72R was from Cabot Co. (Alpharetta, GA). Commercial carbon-supported Pt (20 wt % platinum) was from Johnson Matthey (Ward Hill, MA).

Preparation of catalyst spots.— Catalyst mixtures were prepared on GC supports as described previously.[24] Briefly, a piezoelectric pico-dispenser (Microjet AB-01-60, MicroFab, Plano, TX) was installed onto a digital plotter head (Houston Instruments DMP-5, Houston, TX) to dispense picoliter amounts of metal-salt solutions at programed locations on a glassy carbon substrate by application of 50–60 V pulses (pulse time 25 μs) to the dispenser. Metal-salt solutions typically contained 0.3 M salt in a 3:1 solution of water/
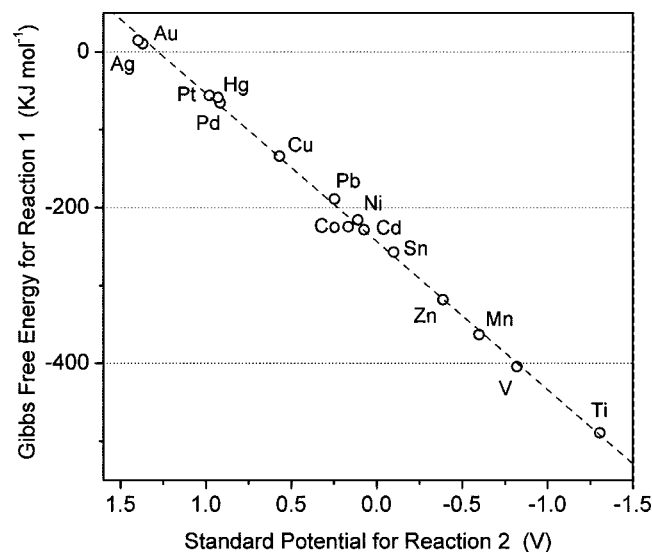
Figure 1. Thermodynamic guidelines for bimetallic catalyst design for ORR (see the text for details) (Ref. 24). Reaction 1. $2M + O_2 \rightarrow 2MO$. Reaction 2. $2M'O + 4H^+ + 4e \rightarrow 2M' + 2H_2O$.

Figure 2. SECM TG-SC images of oxygen reduction activity measured on Au–V arrays in 0.5 M H_2SO_4. Tip-substrate distance = 30 μm, tip current = −160 nA, scan rate = 50 μm each 0.2 s. (A) E_S = 0.1 V vs NHE. (B) E_S = 0.2 V vs NHE. (C) E_S = 0.3 V vs NHE. W_M is the atomic ratio of metal M in the electrocatalyst spot.

glycerol. Voltage pulses were applied using a DAQ board (Keithley Series 500, Cleveland, OH) coupled to a high-voltage dc OP Amp (Burleigh PZ-70, Fisher, NY). After agitation to thoroughly mix the components, reduction of the metal-salt solutions to metal was carried out as follows. $HAuCl_4$ and VCl_2 were dispensed to form the Au–V array and the resulting array was treated with H_2 (1 atm) at 550°C for 1 h. Ag–V arrays were prepared using the same procedure by dispensing $AgNO_3$ and VCl_2 solutions. Pd–Mn and Pd–V arrays were deposited using solutions of $(NH_4)_2PdCl_4$, $Mn(NO_3)_2$, and VCl_2. The precursor spots were reduced by dispensing 10 drops of 10 mM $NaBH_4$ directly onto each spot. The complete array was then rinsed with water and a subsequent thermal treatment under H_2 at 550°C for 1 h was applied.

Rotating disk electrode preparation.— Supported Pd and Pd–V electrocatalysts (20 wt % metal) were prepared on carbon by reduction of metal-salt precursors with $NaBH_4$, and dispersed in Nafion solutions. Initially, 160 mg of Vulcan XC-72R was suspended in 50 mL of water containing sufficient amounts of the salts to produce 40 mg of metal in total. The suspensions were then sonicated for 30 min and 10 mL of 0.1 M $NaBH_4$ solution was added dropwise under continuous stirring. The suspensions were stored overnight to ensure complete reduction of the metal salts. The supported electrocatalysts were then centrifuged at least four times to separate the liquid phase and to wash the solid. The resulting powder was dried at 87°C and then heated under H_2 (1 atm) at 550°C for 1 h in a tube furnace (Barnstead International, Dubuque, IA). Inks of the electrocatalyst-containing powders were prepared by dispersing 8 mg of electrocatalyst in 200 μL of a 1 wt % Nafion solution (Aldrich, Milwaukee, WI) in isopropanol and agitating ultrasonically for 15 min. A drop (0.1 μL) of this ink was deposited on a 1 mm diameter GC RDE and dried for 30 s at 40°C. RDE measurements were performed using a standard three-electrode cell with a carbon rod counter electrode and a Hg/Hg_2SO_4 reference electrode. RDE polarization curves were recorded in O_2-saturated 0.5 M H_2SO_4 at a sweep rate of 1 mV s^{-1}.

SECM screening of electrocatalyst arrays.— Tip generation-substrate collection SECM screening was performed using a CH Instruments model 900B SECM (Austin, TX) as described previously.[15,24] A constant current was applied to the working electrode using a 9 V battery between the working (25 μm Au disk sealed in glass) and auxiliary (Au wire) electrodes. In all experi-
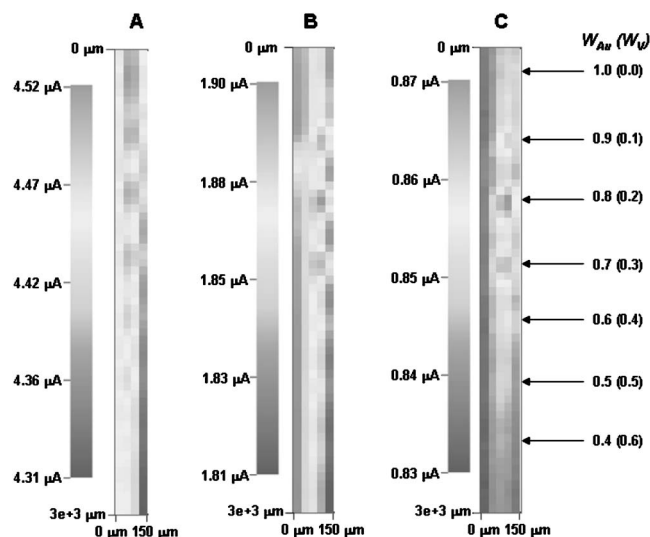
ments a Hg/Hg_2SO_4 reference electrode was used and the potential values reported were adjusted to the normal hydrogen electrode (NHE) scale, where Hg/Hg_2SO_4, H_2SO_4(0.5 M) = 0.65 V vs NHE.

Results and Discussion

SECM ORR activity screening.— Figure 2 shows SECM images obtained upon screening an array containing mixtures of Au and V over a range of substrate potentials, E_S. At E_S = 0.1 V pure Au is active for the ORR and so are electrocatalyst combinations that contain low amounts of V, indicated by essentially the same substrate current (i_S) in the color scale plot (Fig. 2a). Figure 2b and c shows the SECM images recorded for the Au–V array with E_S at more positive potentials. At E_S = 0.2 V (Fig. 2b) the electrocatalytic activity of pure Au is almost zero, while mixtures containing 10–30% V clearly exhibit some activity for the ORR. At E_S = 0.3 V the activity of pure Au is zero and it is possible to distinguish among the activities of those mixtures containing low amounts of V and the mixture containing Au:V at a ratio of 80:20, which exhibits the highest activity for the ORR at this potential.

Figure 3 shows the SECM images recorded for electrocatalyst mixtures containing Ag–V over a range of substrate potentials. Upon screening, the behavior was similar to that observed for the Au–V array. At the most negative potential, E_S = 0.05 V vs NHE (Fig. 3a), pure Ag and those mixtures containing relatively low amounts of V exhibit similar activities. As the substrate potential was made more positive (Fig. 3a and b), the electrocatalytic activity of pure Ag decreased to zero while those combinations containing low amounts of V showed some activity, even at the most positive potential measured, E_S = 0.25 V. Pure Au and Ag are poor electrocatalysts for the ORR and both show significant improvements for the ORR upon mixing with V, although the absolute activities are still inferior to a good electrocatalyst such as Pt. Nevertheless, both of these cases follow the general guidelines proposed for bimetallic electrocatalyst design, i.e., improving the behavior of metal 2 (Au, Ag) by the addition of a metal 1 (V).

As mentioned previously, relatively high electrocatalytic activities for the ORR have been observed for Pd-based mixtures containing small amounts of Co.[24,25] However, the free energy for the formation for CoO is relatively low (−220 kJ mol^{-1}). In this study, a number of metals with much more negative free energies for oxide formation were chosen to combine with Pd. Mn and V have oxide
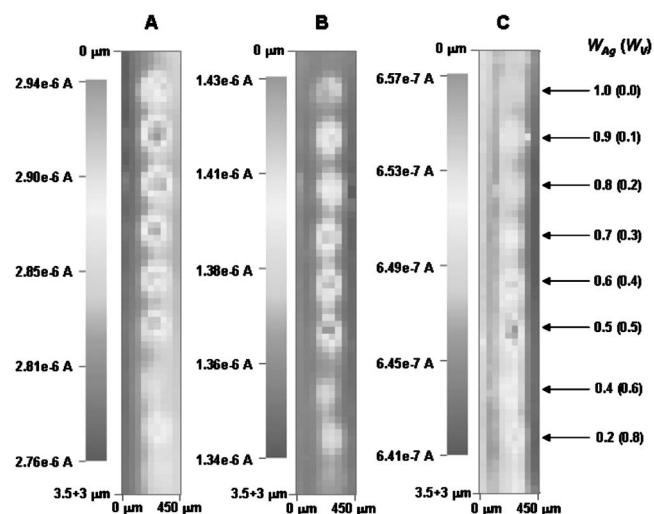
Figure 3. SECM TG-SC images of oxygen reduction activity measured on Ag–V arrays in 0.5 M H$_2$SO$_4$. Tip-substrate distance = 30 μm, tip current = −160 nA, scan rate = 50 μm each 0.2 s. (A) E_S = 0.05 V vs NHE. (B) E_S = 0.15 V vs NHE. (C) E_S = 0.25 V vs NHE. W_M is the atomic ratio of metal M in the electrocatalyst spot.

formation free energies well below −350 kJ mol^{-1} (Fig. 1) and readily promote dissociative chemisorption of O$_2$. Figure 4 shows SECM images recorded for a series of Pd–Mn combinations at different potentials. As E_S was adjusted in a positive potential direction from 0.4 V vs NHE (Fig. 4a), the activity of pure Pd decreased and was almost zero at E_S = 0.6 V (Fig. 3c). The mixture containing 30% Mn showed the highest activity at the most positive potential measured, and the enhancement is comparable to the improvements observed in Ag upon addition of relatively small amounts of V.

Figure 5 shows SECM images recorded for combinations of Pd–V over a relatively wide range of E_S values. Again, at the most negative potential (E_S = 0.3 V, Fig. 5a), almost all of the Pd–V combinations (from 0–60% V) showed activity for the ORR. However, at more positive potentials the activity of pure Pd and those
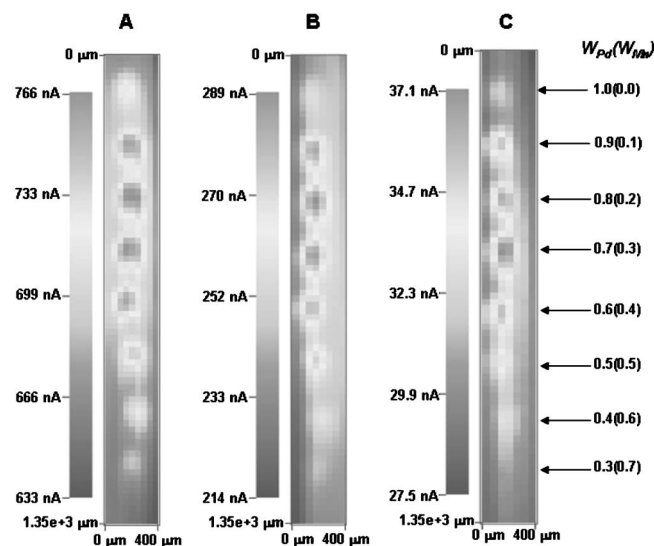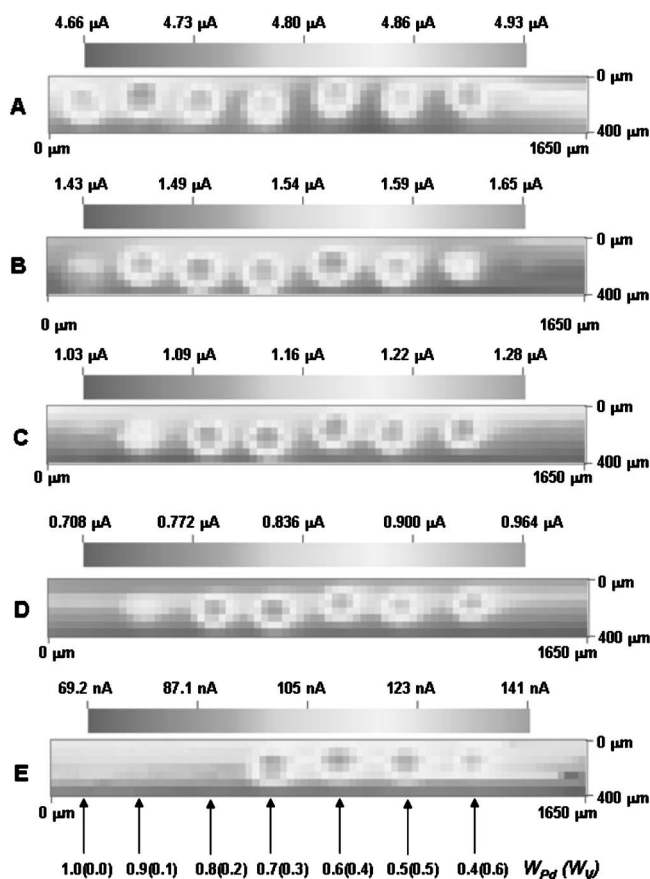

Figure 5. SECM TG-SC images of oxygen reduction activity measured on Pd–V arrays in 0.5 M H$_2$SO$_4$. Tip-substrate distance = 30 μm, tip current = −160 nA, scan rate = 50 μm each 0.2 s. (A) E_S = 0.3 V vs NHE. (B) E_S = 0.5 V vs NHE. (C) E_S = 0.6 V vs NHE. (D) E_S = 0.7 V vs NHE. (E) E_S = 0.8 V vs NHE. W_M is the atomic ratio of metal M in the electrocatalyst spot.

mixtures containing low amounts of V clearly decreased to zero. However, those Pd–V combinations containing 30–60% V still showed ORR activity at E_S = 0.8 V vs NHE, a decrease in the ORR overpotential of approximately 400 mV when compared with pure Pd.

By combining metals such as Pd, Au, and Ag with Co it was possible to enhance the electrocatalytic activity of the metals (Pd, Au, Ag) by 50–100 mV. As shown here, by combining these metals with metals that have more negative free energies for oxide formation, one can enhance the electrocatalytic activity of each metal significantly, up to an almost 400 mV decrease in the overpotential in the case of Pd–V. This effect is illustrated in Fig. 6, in which the ORR overpotential at each pure metal is shown relative to that observed for the optimum bimetallic combination. For clarity, only the overpotential at the best electrocatalytic metal of the combination is shown, i.e., the ORR overpotentials at Ag and Ag–V are shown, but pure V is not shown as it is the poorest electrocatalyst of the mixture. In addition, the overpotentials described in Fig. 6 are the E_S values at i_S = 20 nA (after background current subtraction) at each electrocatalyst spot, subtracted from the thermodynamic cell potential for the ORR, 1.229 V vs NHE.[26]

Using the screening method described here, we also found a number of bimetallic combinations that did not exhibit any synergetic effect upon mixing. These combinations include Ag–Mn and Pd–Cd. Cd has a relatively positive free energy for oxide formation (−228.4 kJ mol^{-1}) and any synergetic effect may be so small that it cannot be resolved using the screening technique. Moreover, the present selection guide relies on alloy formation or nanometer-scale
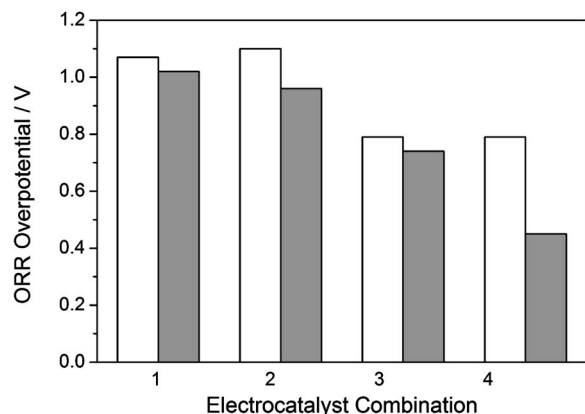

Figure 4. SECM TG-SC images of oxygen reduction activity measured on Pd–Mn arrays in 0.5 M H$_2$SO$_4$. Tip-substrate distance = 30 μm, tip current = −160 nA, scan rate = 50 μm each 0.2 s. (A) E_S = 0.4 V vs NHE. (B) E_S = 0.5 V vs NHE. (C) E_S = 0.6 V vs NHE. W_M is the atomic ratio of metal M in the electrocatalyst spot.

Figure 6. Comparison of the electrocatalytic activities of each pure metal with the corresponding bimetallic electrocatalyst. Colorless bars represent the ORR overpotential at the pure metal and the gray bars represent those at the bimetallic electrocatalysts. The pure metals and combinations are (1) Ag and Ag:V, 50:50, (2) Au and Au:V, 80:20, (3) Pd and Pd:Mn, 70:30, (4) Pd and Pd:V, 60:40.

Figure 7. RDE polarization curves measured by slow potentiodynamic scans (1 mV s^{-1}) of Vulcan carbon-supported commercial Pt (■), Pd–V 60:40 (●), and Pd (○) in O$_2$-saturated (1 atm) 0.5 M H$_2$SO$_4$. Rotation rate: 2000 rpm.

intimate contact between each metal of the bimetallic mixture. Therefore, Pd–Cd and Ag–Mn (which, based on the guide, might be expected to produce a large synergetic effect) are not in intimate contact in the electrocatalytic array spots. This may be due to non-alloy formation in the reduction process. Based on an analysis of the phase diagrams of these combinations,[27] one expects Ag and Mn to form an alloy, however. In the case of Pd–Cd, the phase diagram is quite ambiguous and it is possible that a Pd–Cd phase was not formed using our method. Clearly, the method used to synthesize the electrocatalytic material can have a very large effect on the observed enhanced electrocatalytic activity. For example, Pd–V and Pd–Mn combinations that were prepared only by reduction with H$_2$ at 350°C did not exhibit any synergetic effect. However, as discussed here, when reduced with NaBH$_4$ and then thermally treated under H$_2$, Pd–V and Pd–Mn showed much higher activity than the respective pure metals. These observations suggest that BH$_4^-$ reduction of the salts, which can yield nanoparticles, improves the overall contact between the two metals and at the nanometer scale rapid interdiffusion of the metallic components is possible. Indeed, ready alloy formation from nanometer-size particles is an important advantage of preparation of arrays using these techniques. Issues of particle size and phase formation in ORR electrocatalysis are currently being addressed, and a recent contribution describes these issues in the case of Ti-based electrocatalysts.[28]

RDE activity measurements.— The enhancement of the electrocatalytic activity of Pd upon combining with V, as determined using the SECM screening method, was remarkable and as can be seen in Fig. 5, the mixture containing 40% V exhibited electrocatalytic activity for the ORR at 0.8 V, close to that typically expected only by Pt, some Pt alloys, and some of the previously described bimetallic and trimetallic catalysts. However, the SECM screening method is used as an initial rapid screening technique to identify those materials that appear to show good activity for the ORR. The applicability of rapid automated synthesis and high-throughput screening techniques for novel electrocatalysts has been previously questioned as the structure of deposited metallic arrays may not be comparable to the structure when employed in true fuel cell devices.[29] Therefore, after identification of candidate electrocatalysts that exhibit high activity using the screening method, RDE experiments were used to determine the electrocatalytic activity in configurations that approach more closely those encountered in true fuel cells. To do this, *i-E* curves for 60:40 Pd–V, supported on Vulcan carbon were obtained (Fig. 7). This figure also shows the response obtained for pure Pd as well as Pt, the reference ORR electrocatalyst. Clearly, by
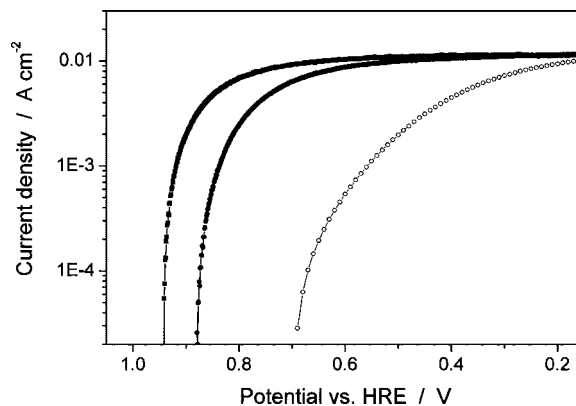
combining Pd with V, the overpotential for the ORR at Pd decreases substantially. At relatively high currents, a decrease in the ORR overpotential of up to 400 mV when compared to Pd is observed, in excellent agreement with the SECM screening observations. Even more significantly, the electrocatalytic activity of Pd has been improved by addition of V to such an extent that, at moderate currents, the difference in overpotentials between pure Pt and Pd–V is less than 100 mV. The observed performance was stable and reproducible for at least 6 days. This aspect may be linked to the fact that V and V alloys easily form surface oxides that passivate the metal and protect it from dissolution. The performance of this material in a membrane electrode assembly (MEA) in a small-scale PEMFC will be evaluated to test the catalyst at high current densities where ohmic effects may be important. Moreover, modifications of the preparation technique may yield electrocatalytic materials with decreased particle sizes with well-defined single phases. Such developments may help to improve even further the activity of these materials.

Conclusions

Based on a previously reported selection guide for the design of improved electrocatalysts for the ORR in acidic media, several additional bimetallic systems have been developed and their electrocatalytic activity probed. Bimetallic arrays were deposited on GC substrate by reduction of metal-salt precursors and electrocatalytic activities were determined using a rapid screening SECM technique. A series of bimetallic combinations that exhibited enhanced electrocatalytic activity when compared with the pure, constituent metals was identified including Au–V, Ag–V, Pd–Mn, and Pd–V. In most cases, the enhancement of electrocatalytic activity was greater than that previously described for Co-based combinations and a greater thermodynamic ability of the V and Mn to break the O–O bond of oxygen to produce the metal oxide may be an important factor. In particular, Pd–V (30 to 60 atom % V) exhibited remarkably high activity for the ORR upon screening, and RDE measurements were used to verify the high activity when the electrocatalyst was supported on Vulcan carbon, i.e., a configuration closer to a fuel cell. Finally, the bimetallic electrocatalyst was compared with Pt and found to exhibit activity remarkably close to that of the commercial electrocatalyst.

Acknowledgments

References

1. C. Song, *Catal. Today*, **77**, 17 (2002).
2. M. Winter and R. Brodd, *Chem. Rev. (Washington, D.C.)*, **104**, 4245 (2004).
3. Q. Li, R. He, J. O. Jensen, and N. J. Bjerrum, *Chem. Mater.*, **15**, 4896 (2003).
4. F. Barbir, *PEM Fuel Cells*, Elsevier, Burlington, MA (2005).
5. H. A. Gasteiger, S. S. Kocha, B. Sompalli, and F. T. Wagner, *Appl. Catal., B*, **56**, 9 (2005).
6. M. A. Hickner, H. Ghassemi, Y. S. Kim, B. R. Einsla, and J. E. McGrath, *Chem. Rev. (Washington, D.C.)*, **104**, 4587 (2004).
7. H. C. Lee, H. S. Hong, Y.-M. Kim, S. H. Choi, M. Z. Hong, H. S. Lee, and K. Kim, *Electrochim. Acta*, **49**, 2315 (2004).
8. C. Wang, M. Waje, X. Wang, J. M. Tang, R. C. Haddon, and Y. Yan, *Nano Lett.*, **4**, 345 (2004).
9. C. A. Bessel, K. Laubernds, N. M. Rodriguez, and R. T. K. Baker, *J. Phys. Chem. B*, **105**, 1115 (2001).
10. H.-F. Cui, J.-S. Ye, W.-D. Zhang, J. Wang, and F.-S. Sheu, *J. Electroanal. Chem.*, **577**, 295 (2005).
11. N. Rajalakshmi, H. Ryu, M. M. Shaijumon, and S. Ramaprabhu, *J. Power Sources*, **140**, 250 (2005).
12. S. Litster and G. McLean, *J. Power Sources*, **130**, 61 (2004).
13. G. J. K. Acres, *J. Power Sources*, **100**, 60 (2001).
14. J. X. Wang, N. M. Markovic, and R. R. Adzic, *J. Phys. Chem. B*, **108**, 4127 (2004).
15. J. L. Fernández and A. J. Bard, *Anal. Chem.*, **75**, 2967 (2003).
16. N. Wakabayashi, M. Takeichi, H. Uchida, and M. Watanabe, *J. Phys. Chem.*, **109**, 5836 (2005).
17. J. R. C. Salgado, E. Antolini, and E. R. Gonzalez, *J. Phys. Chem. B*, **108**, 17767 (2004).
18. U. A. Paulus, A. Wokaun, G. G. Scherer, T. J. Schmidt, V. Stamenkovic, V. Radmilovic, N. M. Markovic, and P. N. Ross, *J. Phys. Chem. B*, **106**, 4181 (2002).
19. H. Yang, W. Vogel, C. Lamy, and N. Alonso-Vante, *J. Phys. Chem. B*, **108**, 11024 (2004).
20. L. Xiong and A. Manthiram, *Electrochim. Acta*, **50**, 2323 (2005).
21. R. Jiang, C. Rong, and D. Chu, *J. Comb. Chem.*, **7**, 272 (2005).
22. S. Guerin, B. E. Hayden, C. E. Lee, C. Mormiche, J. R. Owen, and A. E. Russell, *J. Comb. Chem.*, **6**, 149 (2004).
23. E. Reddington, A. Sapienza, B. Gurau, R. Viswanathan, S. Sarangapani, E. S. Smotkin, and T. E. Mallouk, *Science*, **280**, 1735 (1998).
24. J. L. Fernández, D. A. Walsh, and A. J. Bard, *J. Am. Chem. Soc.*, **127**, 357 (2005).
25. O. Savadogo, K. Lee, K. Oishi, S. Mitsushima, N. Kamiya, and K.-I. Ota, *Electrochem. Commun.*, **6**, 105 (2004).
26. J. P. Hoare, in *Encyclopedia of Electrochemistry of the Elements*, A. J. Bard, Editor, Vol. 2, Chapter II-5, Marcel Dekker, Inc., New York (1974).
27. *Binary Alloy Phase Diagrams*, T. Massalski, H. Okamoto P. R. Subramanian, and L. Kacprzak, Editors, ASM International, Metals Park, OH (1990).
28. J. L. Fernández, V. Raghuveer, A. Manthiram, and A. J. Bard, *J. Am. Chem. Soc.*, **127**, 13100 (2005).
29. B. C. Chan, R. Liu, K. Jambunathan, H. Zhang, G. Chen, T. E. Mallouk, and E. S. Smotkin, *J. Electrochem. Soc.*, **152**, A594 (2005).